# Evaluation of root reinforcement models using numerical modelling approaches

Zhun Mao, Ming Yang, Franck Bourrier, Thierry Fourcaud

# Evaluation of root reinforcement models using numerical modelling approaches

**Zhun Mao · Ming Yang · Franck Bourrier · Thierry Fourcaud**

**Abstract**

*Background and aims* The root reinforcement (RR) models commonly used in slope stability modelling can be simply explained as a single soil additional cohesion parameter estimated with simple analytical functions of root traits. We have simulated 3D direct shear tests using the standard implicit Finite Element Method (FEM) and the Discrete Element Method (DEM), aiming to (i) evaluate the RR models and (ii) compare the two numerical approaches.

*Methods* In homogeneous soil with low cohesion, 36 straight, non-branched and thin root models were implanted in three parallel lines. Root traits, including orientation relative to the shear direction (45°, 90° and −45°), longitudinal modulus of elasticity (10 MPa and 100 MPa), and bending and compressive behaviours (beam, truss and cable) were investigated.

*Results* Compared to the FEM, the DEM achieved consistent results and avoided convergence problems, but required longer computation time and used parameters potentially difficult to identify. Root reinforcement did not occur until significant plastic deformation of soil. The RR values estimated by the shear tests were much lower than those estimated by the usual RR models and were significantly dependent upon root traits.

*Conclusions* Ignoring the effect of root traits in RR models might lead to an important bias when using slope stability models.

**Keywords** Numerical analysis · Direct shear test · Root traits · Root reinforcement · Landslide · Discrete element method · Finite element method

Z. Mao · F. Bourrier (✉)
UR EMGR, IRSTEA,
2 Rue de la Papeterie BP 76, 38402 Saint Martin d'Hères Cedex, France
e mail: franck.bourrier@irstea.fr

M. Yang
UMR 1391 ISPA, INRA,
Aquitaine, 71 Avenue Edouard Bourlaux, CS 20032,
33882 Villenave d'Ornon Cedex, France

M. Yang
Ecole Centrale de Pékin, Beijing University of Aeronautics & Astronautics,
37 Xueyuan Road, Haidian District, 100191 Beijing, People's Republic of China

M. Yang · T. Fourcaud
UMR AMAP, CIRAD,
Boulevard de la Lironde, 34398 Montpellier Cedex 5, France

## Introduction

It is now acknowledged that roots can provide the soil with mechanical reinforcement against various natural hazards, such as shallow landslides, seepage, soil creep etc. (Greenway 1987; Gray and Sotir 1996; Stokes et al. 2009). To quantify and evaluate the effect of root reinforcement (RR) on slope stability, it is of primary importance to understand the mechanical interaction between roots and soil. At a slope scale, RR has been considered a key input when performing stability analysis using either Limit Equilibrium Method (e.g.

*GWEDGEM*, Donald and Zhao 1995; *Slope4Ex*, Greenwood 2006; *BSTEM*, Simon et al. 1999) or Finite Element Method based models (e.g. *ForSLOPE3*, Kokutse 2008; *Ecosfix 1.0*, Mao et al. 2014). In nearly all the previous approaches, the mechanical reinforcement of the soil by the roots was modelled as a single additional cohesion (called "root cohesion", $c_r$) alongside existing soil effective cohesion. This modelling approach allows simplified integration of the roots' impact on slope stability, making stability models easier to compute. The characterisation of $c_r$ has become a research hotspot over the last forty years. A number of authors have developed analytical $c_r$ models in which root cohesion is considered a function of the "tensile strength" of root bundles, e.g. Wu (1976); Waldron (1977); Wu et al. (1979); Pollen and Simon (2005); Thomas and Pollen-Bankhead (2010); Schwarz et al. (2010); Cohen et al. (2011), whilst other authors have used this framework to quantify the spatial-temporal dynamics of $c_r$ at a tree or forest scale, e.g. Schmidt et al. (2001); Sakals and Sidle (2004); Bischetti et al. (2009); Hales et al. (2009); Ji et al. (2012); Mao et al. (2012; 2013).

Nevertheless, the idea of considering the effect of roots as an additional cohesion term has been increasingly challenged by studies conducting soil-roots shear tests at a local scale, i.e. the scale of the root system or root bundle embedded in soil (Abe and Iwamoto 1985; Zhang et al. 2010; Ghestem et al. 2013). Although these studies confirmed the roots' positive reinforcement effect on soil shear strength, they suggested that the strain–stress curve shapes for rooted soils contrasted with those of non-rooted soils. For example, using direct shear tests, Abe and Iwamoto (1985) developed Mohr-Coulomb strength envelope for both non-rooted and rooted soils and found differing slopes, suggesting that roots influence not only cohesion, but also soil friction angle. Similar results were found in Zhang et al. (2010) using tri-axial compression tests. Using direct shear tests on rooted soils, Ghestem et al. (2013) showed that yield soil stress did not necessarily increase with normal load and hence it was impossible to calibrate the parameters of the Mohr-Coulomb criterion and to determine an additional cohesion $c_r$. These findings suggested that the mechanisms by which vegetation roots mechanically interact with soil are far from being fully understood. Moreover, for a given soil type, soil resistance can be influenced by a number of root traits (Reubens et al. 2007; Burylo et al. 2009; Stokes et al. 2009). The root traits may be topological (e.g. architectural organisation of root axes), geometrical (e.g. bundle type, diameter, length, orientation) or mechanical (e.g. tensile strength, modulus of elasticity). These traits can increase the complexity of the interaction between roots and soil, thus making the mechanism of reinforcement more difficult to describe. To investigate the effect of the root traits, many studies have been conducted using techniques such as direct shear tests (e.g. Wu and Watson 1998; Mickovski and van Beek 2009; Mickovski and van Beek 2009; Fan and Chen 2010; Ghestem et al. 2013), pull-out tests (e.g. Mickovski et al. 2007) or tri-axial compression tests (e.g. Zhang et al. 2010) at root bundle (e.g. Mickovski et al. 2007; Zhang et al. 2010) or root system scale (e.g. Wu and Watson 1998; Fan and Chen 2010; Ghestem et al. 2013) using either real roots (e.g. Fan and Chen 2010; Ghestem et al. 2013) or root analogues (e.g. Mickovski et al. 2007). However, although these experimental approaches provide an effective way to study root-soil interaction, they are usually time-consuming and laborious, particularly for generating replicates, considering complex, multiple, and correlated root traits, and controlling environmental factors. Due to the difficulties associated with the experimental approaches, the effects of the root traits on reinforcement have been poorly studied, especially in relation to root geometrical and mechanical traits.

In contrast with experimental tests, numerical tests can constitute a promising alternative for studying roots-soil interaction. Several studies have used standard implicit Finite Element Method (FEM) based numerical methods to simulate processes such as wind induced uprooting and anchorage (Dupuy et al. 2005a, b, 2007; Fourcaud et al. 2008), pull-out (Lin et al. 2010) and direct shear tests (Frydman and Operstein 2001; Mickovski et al. 2011). Despite difficulties in model validation using field data (Dupuy et al. 2007), FEM based tests can be considered reliable numerical approaches generating results which are highly comparable with experimental tests (Mickovski et al. 2011). Recently, a novel rooted soil modelling approach based on the Discrete Element Method (DEM, Cundall and Strack 1979) was developed and showed powerful potential for the exploration of complex root-soil interactions (Bourrier et al. 2013). The DEM based approach models the soil and roots as an assembly of spherical discrete elements and as deformable cylinders, respectively. To the best of our knowledge, however, no studies in the existing literature have yet endeavoured to

compare or examine the complementarities between DEM and FEM models predictions of root-soil interactions.

In this study, we performed three-dimensional direct shear tests using both the FEM and DEM approaches. First, this study aims to explore and compare these two modelling approaches, addressing the following methodological question:

(Q1) What are the advantages, drawbacks and complementarities of standard implicit FEM and DEM?

Secondly,, this study aims at highlighting and quantifying the roots' contribution to soil strength as a function of root traits. The following scientific questions were addressed:

(Q2) How do geometrical (growth orientation, row) and mechanical (modulus of elasticity, modelled root type) root traits affect soil shear resistance?
(Q3) Compared to estimates using existing RR models, can root reinforcement be considered as a single additional cohesion on the basis of Mohr-Coulomb criterion?

## Materials and methods

### Modelling direct shear tests

The direct shear test model developed here is similar to the one developed by Bourrier et al. (2013) which was based on the experimental tests performed by Ghestem et al. (2013). Direct shear tests were preferentially modelled because they constitute classic experiments when exploring the effects of roots on soil resistance. This allows for comparison of different configurations and modelling approaches using similar loading conditions as conventionally used in the literature. It is to be noted that direct shear tests can be considered limited compared with more complex soil mechanics tests, such as triaxial tests. The classic limitations of direct shear tests are mainly related to the following aspects: (i) the distribution of the shear stress at the interface between the two boxes of the shear device, (ii) the relevance of the results obtained at large shear strains, and (iii) the accuracy of measurement at lower/normal pressures.

The model consisted of an upper box (moving box) and a lower box (fixed box) of the same dimensions: 0.5 m (length ($L$), along the $x$-axis)×0.5 m (width ($W$), along the $y$-axis)×0.15 m (height ($H$), along the $z$-axis, Fig. 1a). The walls of the boxes were rigid bodies thus no deformation during the shear process. Soil was homogenous in both boxes. Normal pressure ($\sigma$) were applied at the top of the soil sample. Since the aim of this study is to compare stress–strain relationships between different rooted soils and between different modelling approaches rather than to analyse in detail the yield criterion of the rooted soils, we generally limited the range of explored pressures to two values, i.e. 0.5 kPa and 2.0 kPa, as in Bourrier et al. (2013). Such a low pressure level corresponds to the case where the shear surface of a shallow landslide is located near the soil surface. For each shear test, the upper box was slowly moved in a horizontal direction along the $x$-axis (Fig. 1a), while the lower box was fixed (Fig. 1f). Assuming that a real interface exists between the two half-boxes of the shear device and applying equilibrium equations to the bottom box (Thornton and Zhang 2003), the shear stress at the shear surface between the two boxes can be calculated using the following equations:

$$\tau = (F_R - F_L)/[W \times (L - \gamma)] \quad (1)$$

$$\varepsilon = \gamma/L \quad (2)$$

where, $\tau$ (kPa) and $\varepsilon$ (%) – stress and strain of the soil in the shear box at the shear surface, respectively; $\gamma$ – displacement of the upper box along the $x$-axis; $L$ and $W$ – the length and width of the shear boxes; $F_L$ and $F_R$ – the magnitudes of the contact forces between the soil and the left and right lateral walls of the lower box, respectively (perpendicular to the shear direction, i.e. $x$-axis). This method combines the advantages of the method used in Bourrier et al. (2013) and Ghestem et al. (2013). First of all, using ($F_R - F_L$) instead of the pushing force on the upper box allows the initial contact forces due to soil weight on the lateral faces of the shear box to be taken into account (Thornton and Zhang 2003; Bourrier et al. 2013). Secondly, the term [$W \times (L - \gamma)$] allows the decreasing shear area due to movement of the upper box to be accounted for (Shibuya et al. 1997; Ghestem et al. 2013).

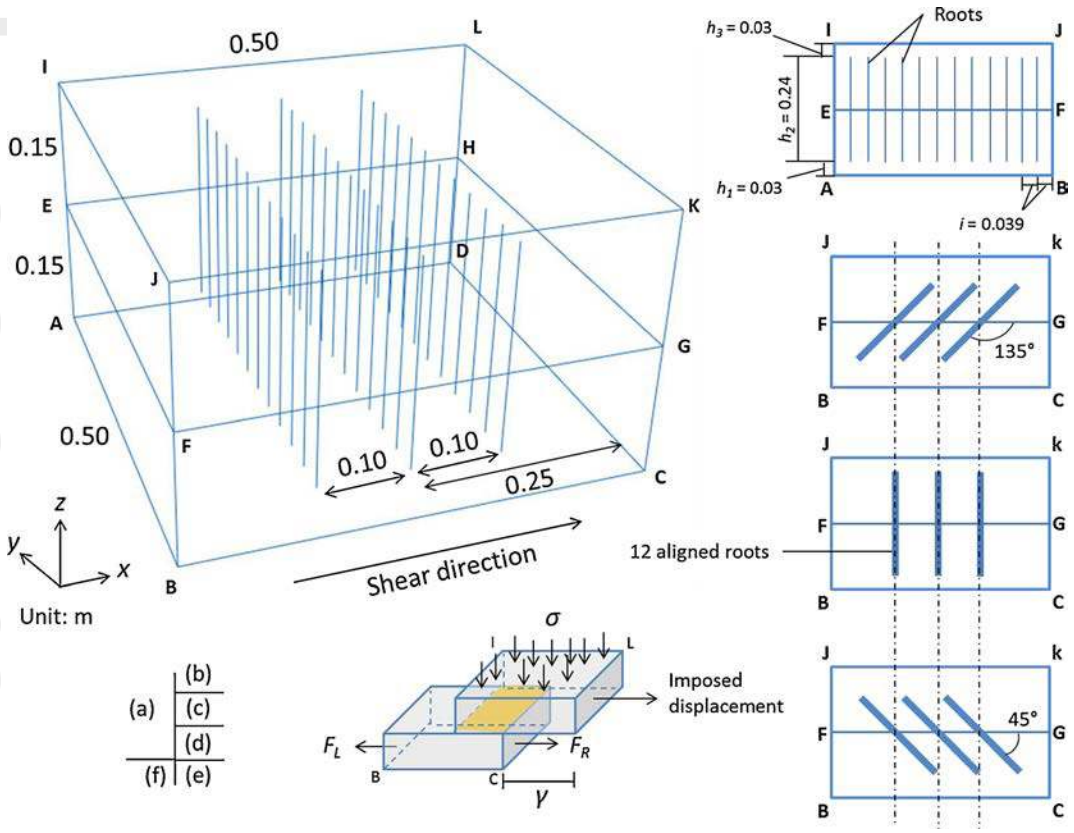


**Fig. 1** Dimensions of shear box and position of embedded roots. (**a**): a global view of an example with 36 vertical roots; the shear direction is along the $x$ axis, from point B to C; boundary conditions of the soil sample are as follows: motion along $y$ axis blocked for the face BCGF, FGKJ, ADHE and EHLI; motion along $z$ axis blocked for the face ABCD; motion along $x$ axis blocked for the face ABFE and CDHG, when the upper shear box moves; (**b**): a cut view in the plane $y$ $z$ with 36 vertical roots; (**c** **e**): cut views in the plane $x$ $z$ with three patterns of root orientations relative to the shear direction (SD: 45° same direction; PD: perpendicular direction; OD: 45° opposite direction ; (**f**): a 3D view of the shear box when shear occurs, see Eq. (1 2) for the meaning of symbols, and the highlighted zone represents the shear area decreasing with increasing shear displacement

## Root properties

In a method similar to that of Mickovski et al. (2011) and Bourrier et al. (2013), straight, non-branched, independent roots were implanted in a parallel, equally spaced fashion into soil (Fig. 1a and b). The number of roots was kept constant in all the tests: 36 roots in 3 rows in the centre of the boxes with an equal interval between rows of 0.1 m (Fig. 1a). Three types of root orientation relative to the upper box displacement direction, i.e. $x$-axis (SD: 45° same direction; PD: perpendicular direction; OD: 45° opposite direction) were tested (Fig. 1c, d and e). Root orientation was the only investigated root geometric trait. Using such a simple root configuration without any connection between the roots enabled us to study the roots' effect and RR model performance without introducing any of the complications of root system architecture. Regarding mechanical traits, we assumed that the basic constitutive material of roots was isotropic (Mickovski et al. 2011; Bourrier et al. 2013) and that root strength and modulus of elasticity in compression were equal to those in tension to facilitate the comparison between the effects of tension and compression loadings. In the simulations, all roots had equal properties. The root tensile strength was set at $T_r$=10 MPa. Two root moduli of elasticity were tested: $E_r$=10 MPa and $E_r$=100 MPa. The choice of these values is consistent with the scope of the published values [see Mao et al. (2012) for $T_r$, and Hathaway and Penny (1975), Fan and Su (2008), Schwarz et al. (2010) for $E_r$]. Root diameter ($d_r$) was fixed at=2 mm. When each root was subject to external forces provided by

mobilised soil, we tested three assumptions for modelling roots:

(i) Beam type roots: roots of this type can sustain tension, compression and bending loadings;
(ii) Truss type roots: roots of this type can sustain tension and compression loadings, but not bending loadings;
(iii) Cable type roots: roots in this type can only sustain tension loadings.

These three structural models cover a wide range of root mechanical behaviours that result from the variability and anisotropy of root cell properties and cell spatial organisation. For example, the beam type root model may represent the "nailing" effect in structural roots, whilst the cable type root model is closer to flexible, fibrous and low-lignified roots that are weak in compression. The truss type model, which may be considered a transitional stage between the beam and cable types, enables us to better understand how the bending, tension and compression loadings in roots contribute to the shear stress of rooted soils.

## Discrete element method based 3D model

The Discrete Element Method based 3D model of direct shear tests was created using the DEM code Yade-Dem (Smilauer et al. 2010). The modelling procedures based on the DEM have been extensively described in Bourrier et al. (2013). Therefore we present only a brief description of the model relevant to this study. The DEM model of direct shear tests considers the soil as an assembly of rigid and locally deformable spheres. Contact forces and moments between spheres were calculated from the displacements between the spheres which accounted for normal and tangential forces at the contact surface between the spheres (Fig. 2). Normal contact forces were calculated using an elastic stress–strain relationship, whereas an elasto-frictional relationship was used for the calculation of tangential forces. Hence, calculation of contact forces depended on three parameters: a local normal modulus, a local tangential modulus and a local friction angle. Regarding the roots, the DEM models each single root as a deformable cylinder similar to an elasto-plastic beam or truss (Fig. 2). Contact forces were also applied between the spheres and the cylinders similarly to sphere-sphere contact forces but with the exception of contact surfaces detection. An elasto-frictional root-soil interface was thus modelled, allowing for root slippage at the interface. The interface friction angle between root and soil spheres was set at the same value as the friction angle between soil spheres, assuming that a slide occurs in the nearest neighbouring soil spheres around the roots and not directly at the interface between roots and the soil matrix, (in line with field observations (Dupuy et al. 2007; Mickovski et al. 2011).

A displacement was slowly effectuated in the upper boxes and the forces on the lateral walls of the bottom box were recorded to calculate the shear stress at the shear surface. The calculation of the shear process during the shear test relied on an explicit solving scheme. For each calculation step, the contact force was first applied to each modelled body (spheres and deformable cylinders). Newton's equations were then solved for each body (Smilauer et al. 2010).

The soil was modelled as an assembly of spheres with diameters of 5 – 8 mm uniformly distributed. This dimension is greater than real soil spheres, but such an assembly is relevant for modelling soil evolution under shear loadings (Bourrier et al. 2013). In order to match the scale of the soil spheres, roots of 12 mm in diameter were used, possessing the same properties (mass, inertia, force-displacement relationship, and maximum admissible tensile force, in particular) as roots of 2 mm (Bourrier et al. 2013). The apparent properties of the soil and roots, i.e. assembly of soil spheres and root cylinders, were dependent on the local contact parameters between soil spheres and cylinders, which are listed in Table 1.

## Finite element method based 3D model

An implicit Finite Element Method (also called "standard FEM") was developed to model direct shear tests, using the software ABAQUS 6.9 (SIMULIA, www.simulia.com). The bare soil was modelled as an elasto-plastic material using the Mohr–Coulomb failure criterion, which is available in ABAQUS and has been used in previous studies on root reinforcement and slope stability (Kokutse 2008; Ji et al. 2012; Mao et al. 2014). The Mohr-Coulomb failure criterion is given by:

$$\tau = c_s + \sigma \tan\phi_s \quad (3)$$

where, $\tau$ – total soil shear stress (kPa), $\sigma$ – effective normal stress (kPa), $\phi_s$ – soil internal friction angle (°), $c_s$ – soil effective cohesion (kPa).

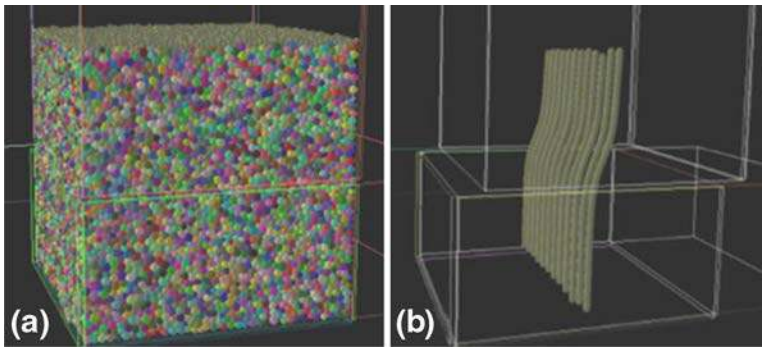


**Fig. 2** Views of the shear box developed using the Discrete Element Method (DEM) after Bourrier et al. (2013). (**a**) and (**b**) are examples of generated soil assembly and root assembly, respectively

The geometry of the soil sample and testing device were similar to those used for the DEM model. In order to make results comparable between the two modelling approaches, we calibrated soil properties in the FEM to obtain similar results for non-rooted soil conditions with those in the DEM available in Bourrier et al. (2013). The chosen soil properties are listed in Table 2. We found that the most appropriate soil friction angle ($\phi_s$) and effective cohesion ($c_s$) to be used in the FEM were 19° and 0.24 kPa, respectively. These values may seem low, however they are representative of natural soils previously tested and comparable to published data [see Preti and Giadrossich (2009) for a case of $\phi_s$ =20° and $c_s$ =1 kPa]. In order to verify if using this weak soil can generate representative results, we also made simulations using a soil of $\phi_s$ =30° and $c_s$ =0.24 kPa (sandy soil) to assess the influence of soil properties on the root reinforcement.

The soil sample was meshed using 3D deformable tetrahedral elements with four nodes, the interval between two nodes being 0.020 – 0.025 m. Each embedded root was discretised using two types of elements: beam elements and truss elements. Using such elements, an elastic stress–strain relationship was applied to the roots until root failure occurred. The geometrical and mechanical properties of a single root are presented in Table 3. Roots were meshed using nodes with an interval of 0.01 m. To put roots in the soil, we used the "EMBEDDED" technique, which is an available option of constraint setting in ABAQUS. According to this technique, if a node belonging to an embedded object (root) is within a host element (soil), the transitional degrees of freedom of the node (termed the "embedded node") are constrained to the interpolated values of the corresponding degrees of freedom of the host element. Nevertheless, rotational degrees of freedom of an embedded node are not constrained by those of the host element. This technique relies on the assumption that root slippage does not directly occur at the root-soil interface but in the nearest neighbouring soil particles around the roots. This means that the root-soil interface is "stronger" than the soil itself in the tangential direction (Mickovski et al. 2011). This is in line with the modelling of root-soil interface in the DEM approach. Beam type roots were modelled using beam elements (B31) available in the ABAQUS element library. They

**Table 1** Parameters used in the discrete element method based model (Here symbols are consistent with those in Bourrier et al. (2013) and see this paper for more details)

| Category | Term | Symbol | Value |
|---|---|---|---|
| Sphere spheres and sphere cylinders | Normal local modulus | $E_n$ | 5 MPa |
| Contact force | Local Poisson's ratio | $\alpha$ | 0.3 (dimensionless) |
| | Local friction angle | $\varphi_c$ | 30 ° |
| Cylinders | Tensile modulus | $E_{ct}$ | 10 100 MPa |
| | Bending modulus | $E_{cb}$ | 0 75 MPa |
| | Local Poisson's ratio | $\alpha$ | 0.3 (dimensionless) |
| | | $\varphi_c$ | 30 ° |
| | Tensile strength | $\sigma_{n,l}$ | 10 MPa |
| | Shear strength | $\sigma_{s,l}$ | 10 MPa |

**Table 2** Mohr Coulomb criterion based mechanical properties of the soil used in the Finite Element Method based model

| Term | Symbol | Value |
|---|---|---|
| Volumic mass | $\rho_s$ | 1,400 kg m $^{3}$ |
| Modulus of elasticity | $E_s$ | 0.32 MPa |
| Poisson's ratio | $p_s$ | 0.33 (dimensionless) |
| Cohesion yield stress | $c_s$ | 0.24 kPa |
| Absolute plastic strain | $\varepsilon_{ps}$ | 0 (dimensionless) |
| Friction angle | $\varphi_s$ | 19° |
| Dilation angle | $\theta_s$ | 0° |

account for factors from root resistance to tension, compression, shear, bending and twisting loadings. Truss type roots were modelled using truss elements (T3D2) that only offer resistance against translational loadings (tension/compression and shear loadings). Cable type roots were modelled using truss elements that are only able to sustain tension loadings. The rotation around the $z$-axis of embedded root nodes within adjacent soil nodes was disabled to prevent self-spinning during the shear process.

## Estimation of root reinforcement

We compared the root additional shear stress $\tau_r$, (kPa) obtained from numerical direct shear tests with that estimated using common RR models. A $\tau_r - \varepsilon$ curve, was determined by subtracting the simulated response curve of the non-rooted soil from the simulated response curve of the reinforced soil.

The component $c_r$ of the RR models based on the Mohr-Coulomb failure criterion (Eq. 3) was added to the bare soil cohesion $c_s$. The most widely used RR models can be divided into two families according to different root breakage patterns (Ji et al. 2012): the Wu's and Waldron's Models "WWMs" (Wu 1976; Waldron 1977) with simultaneous root breakage and the Fibre Bundle Models "FBMs" (Pollen et al. 2004; Thomas and Pollen-Bankhead 2010; Schwarz et al. 2010) with progressive root breakage.

The generic form of WWM (named as "generic WWM") can be expressed as:

$$c_r = 1000 \times [\sin(90° - \psi) + \cos(90° - \psi)\tan\phi_s] \times F_r \quad (4a)$$

$$F_r = \sum_{n=1}^{N} \frac{\pi T_{rn} d_{rn}^2}{4A_s} \quad (4b)$$

where, 1000 – the convertor from MPa to kPa; $F_r$ – total mechanical tensile contribution of the roots (Pa); $N$ – total number of roots, and $N$=36 (as chosen for this study); $T_{rn}$ – maximum tensile strength (MPa) of the root $n$, $n \in [1,N]$; $d_{rn}$ – diameter of the root $n$ (mm); $A_s$ – soil area where roots were counted (m$^2$), $A_s = L \times W$; $\psi$ – angle of the root at rupture relative to the failure plane (°), $\psi \in [0°, 180°]$. Roots are in a position of tension when $\psi \in [0°, 90°]$ and of compression when $\psi \in ]90°, 180°]$. Gray and Ohashi (1983) claimed that randomly oriented roots generated similar $c_r$ to perpendicular roots, suggesting that Eq. (4b) can be used for root compression position. Alternatively, Wu and Watson (1998) and Thomas and Pollen-Bankhead, (2010) proposed calculation of the roots' buckling load based on the Euler method, rather than a compression load. The root buckling stress ($B_{rn}$, MPa) can be calculated by:

$$B_{rn} = 10^6 \frac{\pi^2 d_{rn}^2 E_{rn} \sin^2\psi}{16\mu z^2} \ (\psi \in ]90°, 180°] \ ) \quad (5)$$

where, $E_{rn}$ – modulus of elasticity of the root $n$ (MPa); $z$ – thickness of shear zone (m); $\mu$ – column effective length factor, $\mu$=1 (chosen since roots are considered as pinned piles). When considering the buckling process, $T_{rn}$ in Eq. (4b) should be replaced by $B_{rn}$ in Eq. (5). $\psi$ in Eq. (4a) and Eq. (5) can be estimated by:

$$\psi = \tan^{-1}\left(\frac{1}{\tan\theta + 1/\tan i}\right) \quad (6)$$

where, $i$ – initial root orientation relative to the failure plane(°), $i \in [0°, 180°]$ and thus $i$ can be 45° (SD), 90°

**Table 3** Geometrical and mechanical properties of a single root used in the Finite Element Method based model

| Term | Symbol | Value 1 | Value 2 |
|---|---|---|---|
| Form | Cylinder | | |
| Length | $l_r$ | 0.24 m | |
| Diameter | $d_r$ | 2 mm | |
| Volumic mass | $\rho_r$ | 900 kg m $^{3}$ | |
| Modulus of elasticity | $E_r$ | 10 MPa | 100 MPa |
| Poisson's ratio | $p_r$ | 0.33 (dimensionless) | |
| Yield stress | $T_r$ | 10 MPa | |
| Plastic strain | $\varepsilon_{pr}$ | 0 (dimensionless) | |

(PD) and 135° (OD); $\theta$ – angle of shear distortion (°) and can be obtained using Eq. (7):

$$\tan\theta = \frac{\Delta U_{rx}}{z} = \frac{U_{rx1} - U_{rx0}}{z} \quad (7)$$

where, $\Delta U_{rx}$ – root displacement (m) along the shear direction ($x$-axis) until breakage, calculated by the final root position, $U_{rx1}$, subtracting its initial position, $U_{rx0}$. Although relatively high and variable values of $\theta$ have been chosen in a number of studies (see a review in Thomas and Pollen-Bankhead 2010), Docker and Hubble (2008) found that $\theta$ was quite small, ranging from 1° to 25°, and that the estimated values of $\theta$ based on measurement of four Australian riparian tree roots were no more than 10°. Estimates from our FEM simulations showed that before computational divergence, $z$ had a value of approximately 0.08 m (non-rooted condition) – 0.2 m (rooted condition) and $\Delta U_{rx}$ was relatively small for all the rooted cases, i.e. c.a. 0.002 m–0.01 m (data not shown). Hence, we obtain small values of $\tan\theta$ in accordance with Docker and Hubble (2008). According to Eq. (6), $i$ could be used as an approximate estimate of $\psi$, as in Danjon et al. (2008). The term $[\sin(90°-\psi)+\cos(90°-\psi)\tan\phi_s]$, known as the root orientation factor (ROF), controls the efficiency of root reinforcement due to tensile strength (Gray and Leiser 1982). Sensitivity analyses in Danjon et al. (2008) and Thomas and Pollen-Bankhead. (2010) showed that the absolute value of the ROF was highly variable ranging from 0.0 to 1.4 as a function of $\theta$, $i$ and $\phi_s$, even for cases where $\theta$ is small with little variation (as is the case for this study). However, in practice, the ROF tends to be assigned fairly constant values, probably due to the difficulties in in situ measurement of $\theta$ and $i$. Most of the chosen ROF in the literature are close to 1.0 (Thomas and Pollen-Bankhead 2010). The most classic value is 1.2, which was proposed by Wu et al. (1979). With this value, the generic WWM, i.e. Eq. (4a) and (4b), for estimating $c_r$ (kPa) thus becomes:

$$c_r = 1200 \times \sum_{n=1}^{N} \frac{\pi T_{rn} d_{rn}^2}{4A_s} \quad (8)$$

Eq. (8) (named "simplified WWM") was initially thought to be only suitable only for the case of perpendicular roots embedded into highly frictional soils ($\phi_s >$ 35°, Wu et al. 1979; Greenway 1987). However, due to the simple model design and small parameter number, ROF=1.2 in Eq. (8) has been widely used since its naissance (Bischetti et al. 2005; Mattia et al. 2005; Reubens et al. 2007; Genet et al. 2008, 2010; Mickovski and van Beek 2009; Mickovski and van Beek 2009). In order to simplify the model and simultaneously overcome the overestimation of Eq. (8), Preti and Schwarz (2006) introduced a correction factor $k''$= 0.4 to Eq. (8) leading to Eq. (9) (named "Preti-Schwarz WWM" for estimating $c_r$ (kPa):

$$c_r = 480 \times \sum_{n=1}^{N} \frac{\pi T_{rn} d_{rn}^2}{4A_s} \quad (9)$$

Besides the WWMs, a series of FBMs have been introduced to estimate $c_r$ (Pollen and Simon 2005; Thomas and Pollen-Bankhead 2010; Schwarz et al. 2010). The FBMs possess the same Eq. (4a) as the WWMs but differ in Eq. (4b). Instead of accumulating the tensile force of all the roots (i.e. simultaneous breakage), the FBMs impose successive root breakage which better reflects field observations. Amongst the four FBMs used in the present study, three of them use load as the driving factor determining the root breaking order, but they differ in terms of load distribution hypotheses: each root is subjected to (i) the same force regardless of root diameter or cross-sectional area (named "FBM, by load"); (ii) the force that is proportional to the ratio of its diameter to the sum of the diameters of all the roots (named "FBM, by diameter") and (iii) the force that is proportional to the ratio of its cross-sectional area to the sum of the cross-sectional areas of all the roots (named "FBM, by stress"). Additionally, Schwarz et al. (2010) presented a new FBM in which root breakage was determined by root strain, instead of load (named "FBM, by strain").

We estimated the RR using the seven models, i.e. generic WWM; simplified WWM; Preti-Schwarz WWM; FBM, by load; FBM, by diameter; FBM, by stress; FBM, by strain. To facilitate the use of FBM algorithms, a randomisation was conducted for diameter ($2\pm2\times\Delta$) mm [where, $\Delta$ is the amplitude of variation in percentage (%), *idem.* for the following cases], tensile strength ($10\pm10\times\Delta$) MPa and modulus of elasticity ($100\pm100\times\Delta$ and $10\pm10\times\Delta$) MPa for the 36 roots, instead of using a linear interpolation method, as in Pollen and Simon (2005), Thomas and Pollen-Bankhead (2010), and Mao et al. (2012). Sensitivity analysis was carried out to investigate the impact of $\Delta$ on $c_r$-estimates. For each range of variation ($\Delta \in [1,99]$), randomisation was applied for each root property and

100 simulations were run. For OD orientated roots, both compression processes (with buckling and without buckling) were tested.

Theoretically, the $c_r$ estimated by the four FBMs can be variable with increasing soil strain, with which root breakage is supposed to be progressive, especially for the "FBM, by strain" model in Schwarz et al. (2010). However, we did not obtain root breakage – soil strain curves, as all the roots in our study were not broken. Following Ji et al. (2012), we only calculated constant values of RR estimates at root tensile strength when using the FBMs.

## Results

### Root additional cohesion estimated by RR models ($c_r$)

The sensitivity analysis (Fig. 3) showed that increasing $\Delta$ significantly increased the standard deviation of $c_r$ estimated by all the RR models. The evolution of $c_r$ with increasing $\Delta$ differed between the RR models. The $c_r$ values estimated by the WWMs were initially stable but rapidly increased after $\Delta$=20 %, whereas those estimated by the FBMs showed "U" shaped evolution. Amongst the RR models possessing the same ROF, the order of prediction remained almost unchanged regardless of $\Delta$ ranging from 5 % to 95 %, and the $c_r$ values estimated by the FBMs were closely related to those estimated by the generic WWM. In the case of SD oriented roots, the simplified WWM and Preti-Schwarz WWW tended to give the maximum and minimum $c_r$-estimates, respectively. For OD oriented roots, compression with buckling generated insignificant $c_r$, approximately two orders of magnitude lower than $c_r$ without buckling (Fig. 3a and d).

### Soil shear stress ($\tau$) – soil strain ($\varepsilon$) curves

The soil parameters for the FEM model were calibrated in order to obtain similar curves to those obtained using the DEM model (Fig. 4). The plateau values of $\tau$ obtained for shear stress using both approaches almost overlapped. However, the curves obtained using the

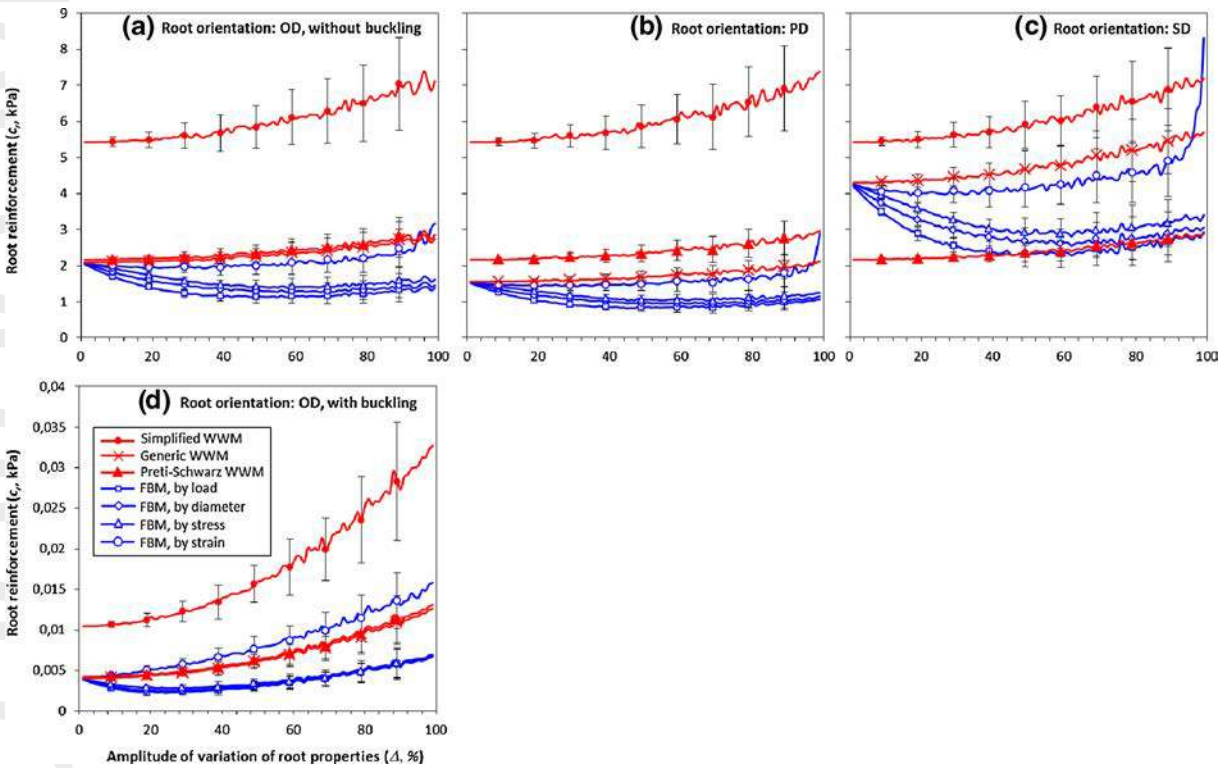


**Fig. 3** Sensitivity analysis of $c_r$ estimates (mean ± standard deviation) using RR models according to the amplitude of variation of root properties, i.e. diameter, tensile strength, modulus of elasticity. For modulus of elasticity, here only the case of $E_r$ = 100 MPa is shown. Root orientations relative to the shear direction (OD: 45° opposite direction; PD: perpendicular direction; SD: 45° same direction. Error bars are only shown for the $x$ axis=9$m$ ($m$ in [1, 8])

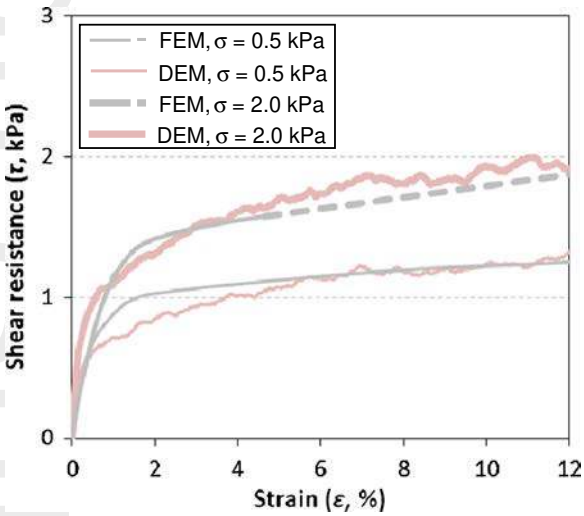


**Fig. 4** $\tau$ $\varepsilon$ curves of direct shear test for non rooted soils using the standard Finite Element Method (FEM) based model and the Discrete Element Method (DEM) based model. $\sigma$ normal pressure (kPa)

two different approaches differed slightly (Fig. 4). At very low strains (approximately <0.2 %), the increase in the shear stress was larger with the DEM approach, meaning that he DEM sample was stiffer. Additionally, the transition from the initial rapid increase in shear stress to a plateau was more progressive for the DEM-based sample.

According to the FEM-based tests, the shape of the $\tau - \varepsilon$ curves for $\varepsilon$ <1.5 % remained almost unchanged for non-rooted and rooted soil samples, regardless of the simulation scenario (Figs. 5 and 6). The shape disparity of $\tau - \varepsilon$ curves occurred when $\varepsilon$ >1.5 % according to the different root traits tested (from here on we will call the turning point at $\varepsilon$ <1.5 % the "yield point"). Convergence problems often occurred in the FEM based $\tau - \varepsilon$ curves, especially when $\varepsilon$>4.0 %, whereas these problems were not found when using the DEM. All the $\tau - \varepsilon$ curves exhibited a linear relationship with increasing $\varepsilon$ for $\varepsilon$ >1.5 % (Figs. 5 and 6). When the root modulus of elasticity ($E_r$) was low (10 MPa), the OD orientated roots showed very limited shear stress, which was comparable to that of nonrooted cases (Fig. 5a and b). Except for the OD orientation, roots with $E_r$=100 MPa were more efficient in increasing $\tau$ compared to roots of $E_r$=10 MPa. This tendency was particularly remarkable for the SD orientation (Fig. 5e and f). The OD orientated roots showed the lowest capacity for soil reinforcement (Fig. 5a and b).

For the PD (Fig. 6c and d) and SD (Fig. 6e and f) oriented roots, all the root types (beam, truss and cable) generated fairly similar $\tau - \varepsilon$ curves. For the OD orientation, cable type roots provided non-effective reinforcement and their $\tau - \varepsilon$ curves almost overlapped with the curve for non-rooted soil (Fig. 6a and b). Truss type roots in OD orientation were as efficient as beam type ones for $\varepsilon$<4.0 %, however we observe a drop in $\tau$ value followed by an increase at $\varepsilon$>8.0 % (Fig. 6a and b).

The results from the DEM simulations generally led to similar qualitative conclusions to those from the FEM simulations regarding root reinforcement as well as the influence of $E_r$ and root type (Fig. 7). However, difference between rooted and non-rooted soil simulations could not be clearly observed until $\varepsilon$ >10.0 % using the DEM approach (Fig. 7), much later than for the FEM (i.e. $\varepsilon$ >1.5 %) (Figs. 5 and 6).

## Spatial distribution of strains in the soil sample

Focusing on the configuration for which root reinforcement is the most efficient (i.e. the SD orientation and beam type roots) and according to the standard FEM simulations, the location and magnitude of plastic strains, potentially associated with soil failure, were significantly influenced by the presence of roots and their associated traits (Fig. 8). For non-rooted soils, the plastic zone first occurred on the left side of the interface between the two shear boxes (Fig. 8a). Then, this zone progressively extended throughout the whole classically assumed shear surface and formed a typical "belt-shaped" plastic zone (Fig. 8b). During this process, no failure occurred in the soil that was distal to the interface (Fig. 8a and b). For rooted soils, the plastic zone also initially occurred on the left side of the box interface. Upon reaching root rows, the plastic zone tended to preferentially propagate in the vertical direction, i.e. perpendicular to the classically assumed shear surface (Fig. 8c, d and e). The plastic zone was thus concentrated on the left side of the roots (Fig. 8c, d and e). It is to be noted that the shape and surface of the failure zone depended on the orientation of the roots. Beam type roots in the SD orientation generated a larger failure zone than roots in the OD orientation. When root reinforcement was not effective, i.e. in case of cable type roots in the OD orientation, the failure zone was identical to that of non-rooted soils (Fig. 8a and b).

## Root deformation

Roots in the three rows showed contrasted axial (i.e. the roots' longitudinal) strain evolution during the shear process (Figs. 9 and 10). Focusing on the results from the

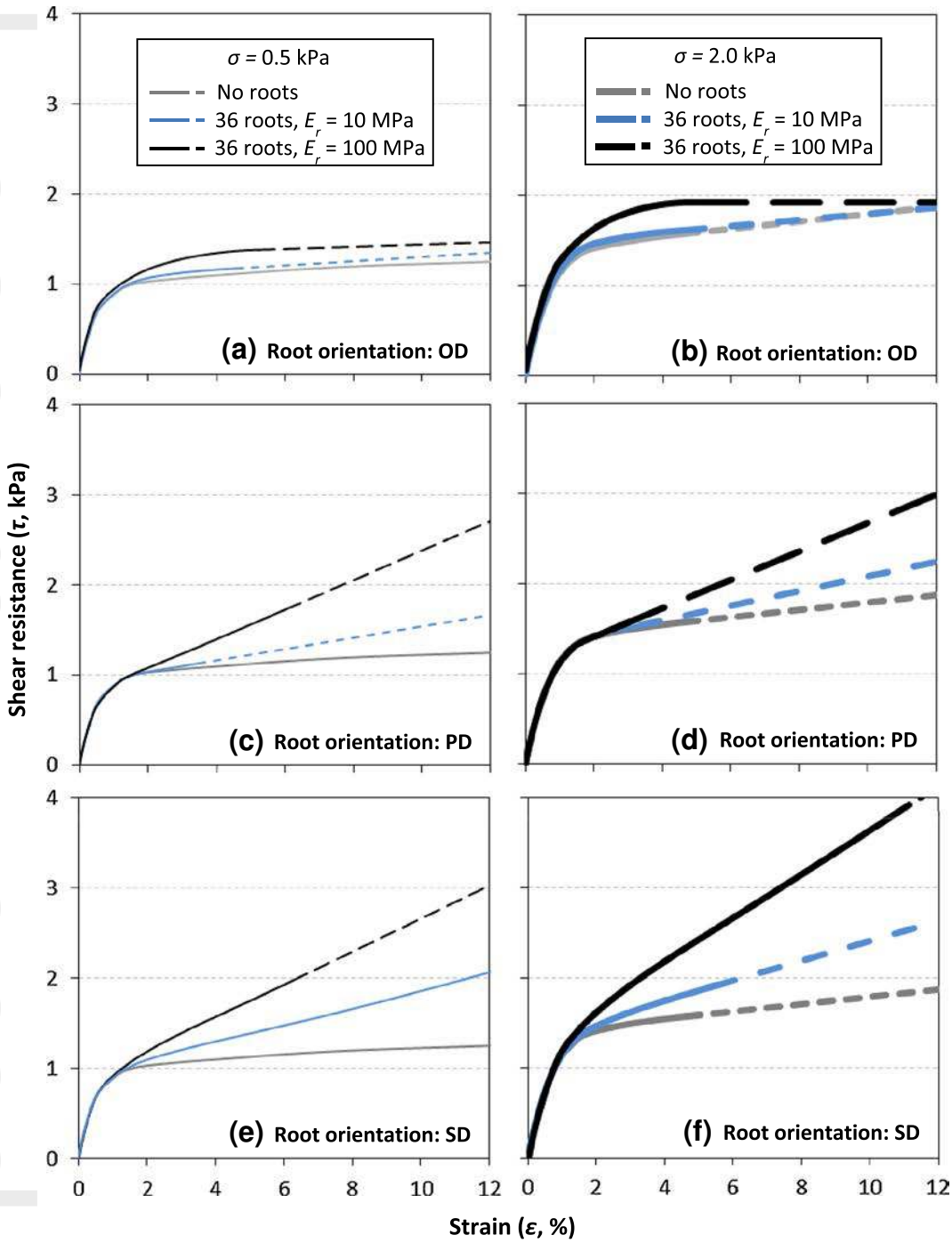


**Fig. 5** $\tau$ $\varepsilon$ curves of direct shear test on the basis of the standard Finite Element Method for different normal pressure ($\sigma$, 0.5 kPa; 2.0 kPa), root orientations relative to the shear direction (OD: 45° opposite direction; PD: perpendicular direction; SD: 45° same direction), and root modulus of elasticity ($E_r$, 10 MPa; 100 MPa). Roots were modelled as beam elements. If a simulation did not reach convergence, a dashed line was added following the curve tendency at its distal part to better indicate the tendency

standard FEM simulations, roots in the left row were the most heavily loaded by the mobilised soil and thus showed the largest strain values (Fig. 9). Amongst the three types of root orientation, only roots in the OD orientation showed compression strains (Fig. 9). The evolution of root strains was

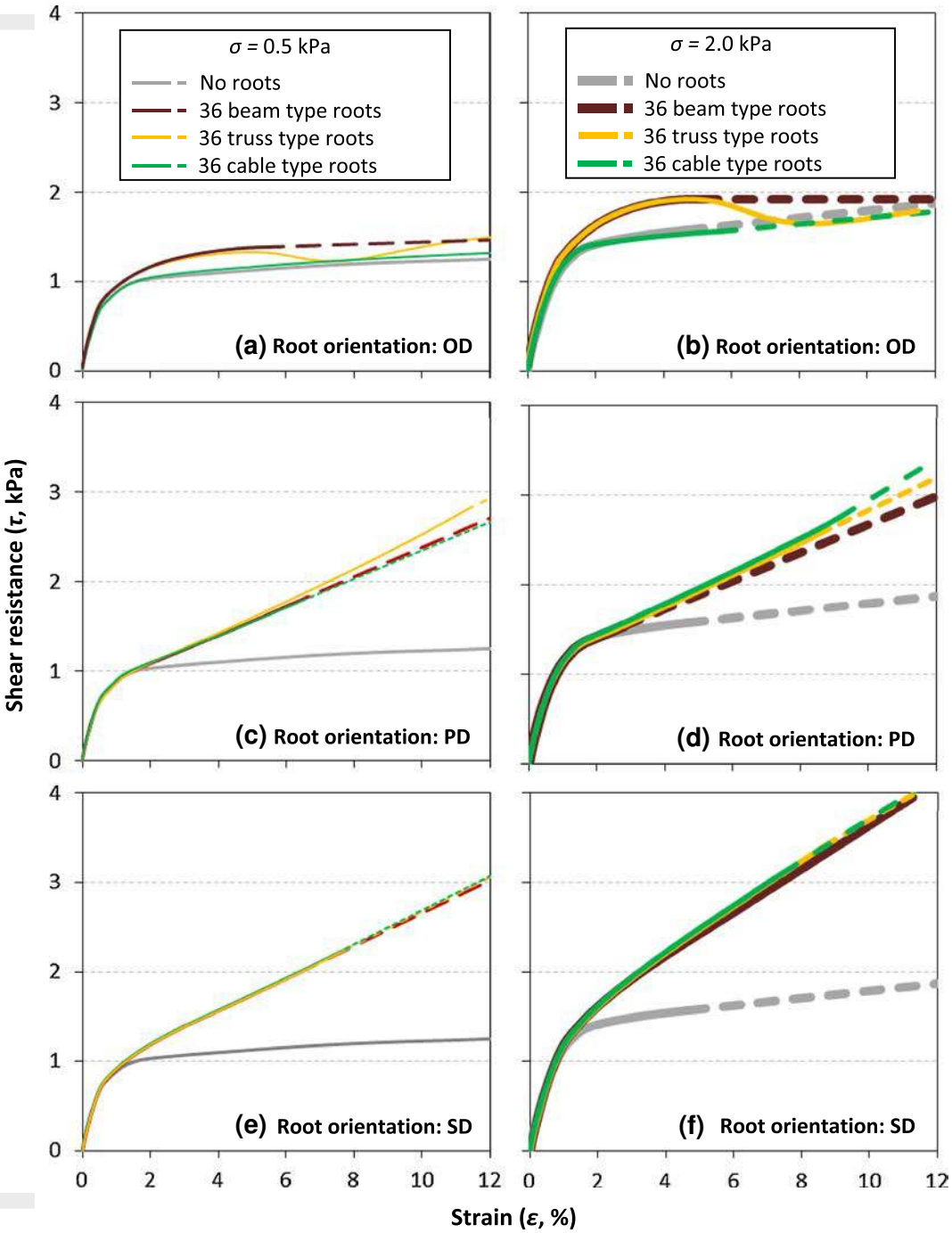


**Fig. 6** $\tau$ $\varepsilon$ curves of direct shear test on the basis of the standard Finite Element Method for different types of roots (beam; truss; cable) and root orientations relative to the shear direction (OD: 45° opposite direction ;PD: perpendicular direction; SD: 45° same direction). For all the curves, the root modulus of elasticity ($E_r$)= 100 MPa. If a simulation did not reach convergence, a dashed line was added following the curve tendency at its distal part to better indicate the tendency

significantly influenced by root orientation and root model type (Fig. 11). Roots of beam type showed almost linear increase in axial strain (and also root stress) with increasing soil strain (Fig. 11a) regardless of root orientations. For cable type roots in the OD orientation subjected to

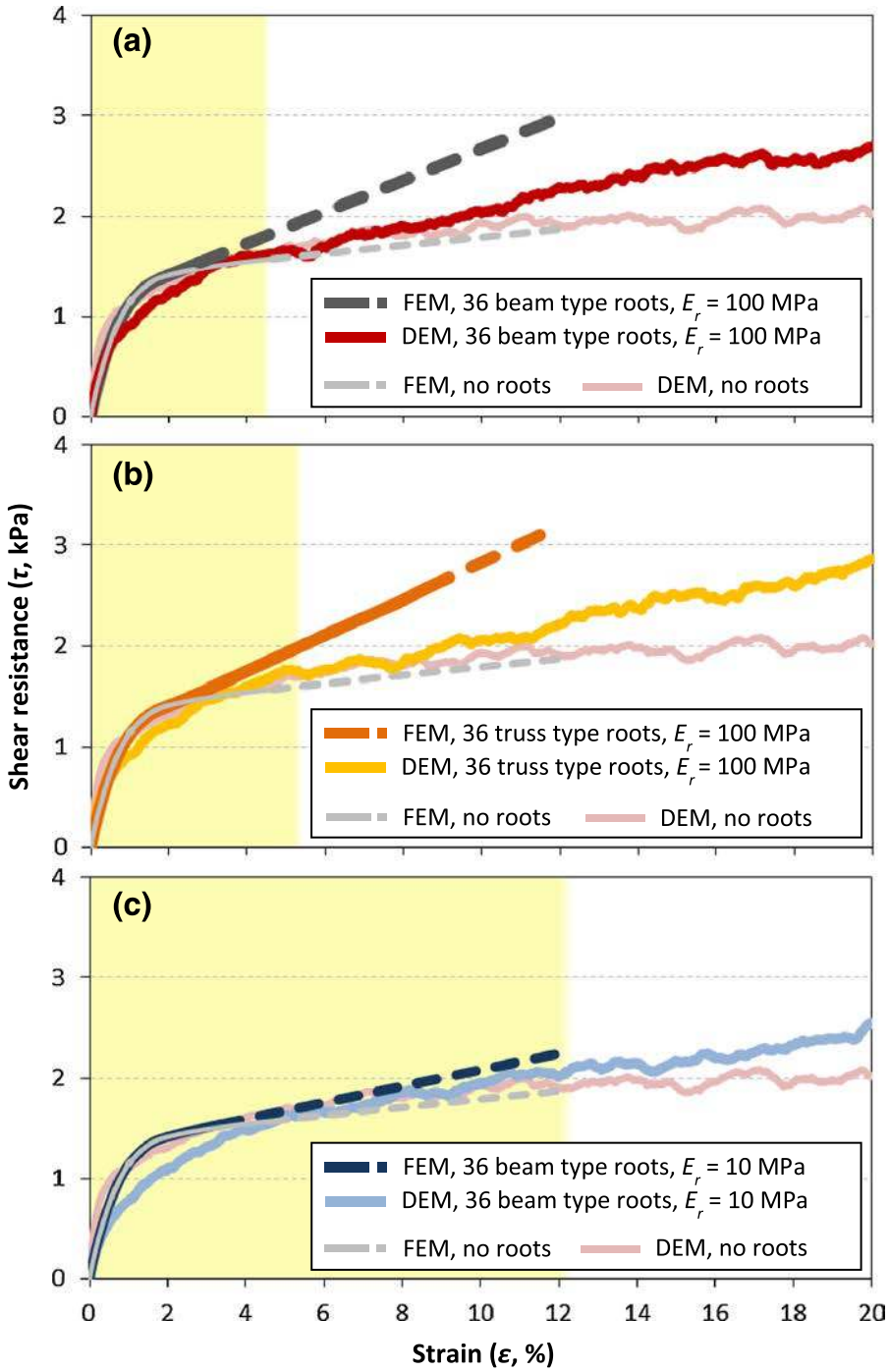


**Fig. 7** Comparison of $\tau$ $\varepsilon$ curves of direct shear test between FEM and DEM based models. Root orientation is perpendicular to the shear direction (PD) and $\sigma$=0.5 kPa for (**a c**). Shadow zone denotes the scope of strain in which $\tau$ in the standard FEM simulations and that in the DEM simulations were comparable ($\tau$<c.a. 0.3 kPa). If a simulation did not reach convergence, a dashed line was added following the curve tendency at its distal part to better indicate the tendency

compression loadings, the axial strains sharply decreased (Fig. 11c) as they offered no resistance to compression loadings. When truss type roots were subjected to compression loadings, their axial

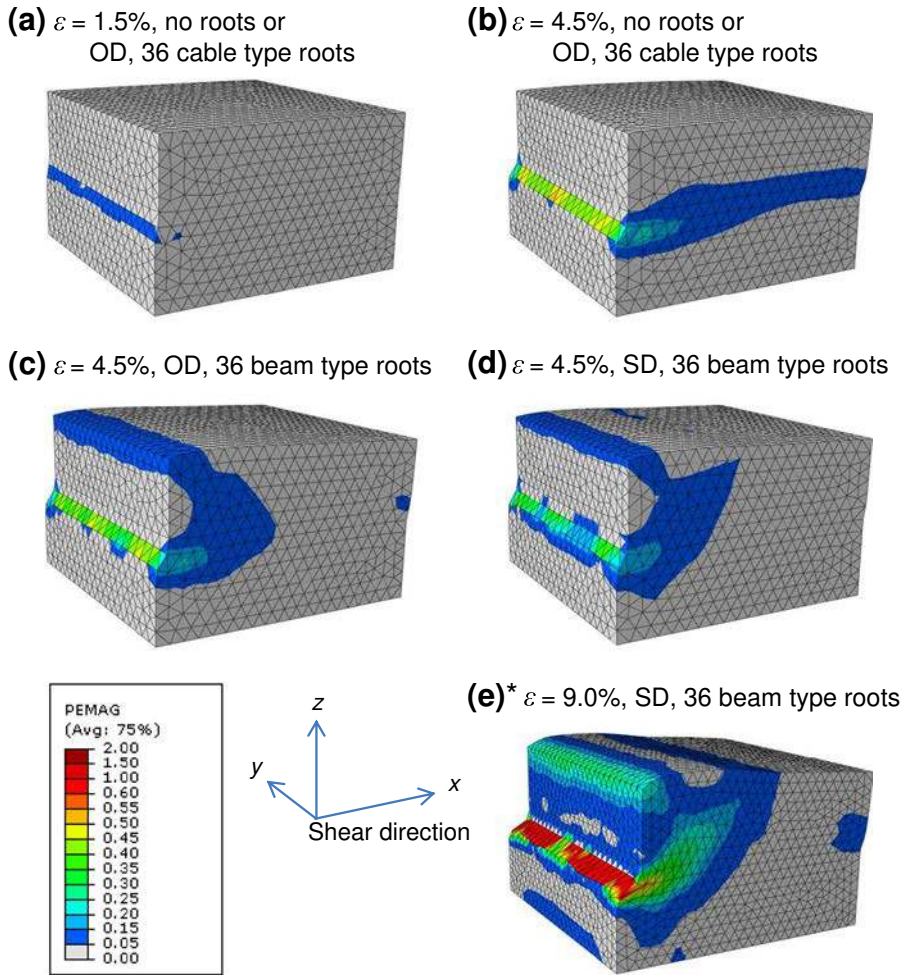


**Fig. 8** Visualisation of soil plastic strains for non rooted and rooted soils. PEMAG plastic strain magnitude; *: a seed density of 0.020 m in mesh was used rather than a density of 0.025 m

strain evolution with shear strain exhibited a "U" shaped curve (Fig. 11b). Finally, DEM simulation results showed a similar effect for root rows (Fig. 10), in particular for very large strains (Fig. 10c and d). In all the simulation scenarios, none of the roots were broken when the soil had already failed or plastified (i.e. simulation divergence), as the axial strain of all the roots with $T_r$=10 MPa and $E_r$=100 MPa did not exceed 10 % (Fig. 11).

Root additional shear stress ($\tau_r$) – soil strain ($\varepsilon$) curves

In the standard FEM results, $\tau_r$ was not constant during the shear process, but varied as a function of soil strain (Fig. 12). In general, root orientation more significantly influenced $\tau_r - \varepsilon$ curves than root type in terms of both the value of $\tau_r$ and curve shape (Fig. 12a, b and c). SD orientated roots provided the largest reinforcement (Fig. 12c), whereas OD orientated roots provided the lowest reinforcement, especially for cable type roots (Fig. 12a).

A significant difference was found between $\tau_r$ from shear testing and $c_r$ obtained from the RR models, even between the $c_r$ values estimated by the RR models themselves (Fig. 12). The simplified WWM provided higher $c_r$-estimates compared to the highest values of simulated $\tau_r$ obtained at high soil strain. This was true even for the Preti-Schwarz WWM, which is supposedly the most conservative model (Fig. 12). For OD orientated roots, compression with buckling and without buckling underestimated and overestimated the RR respectively (Fig. 12a). In general, normal pressure had a significant

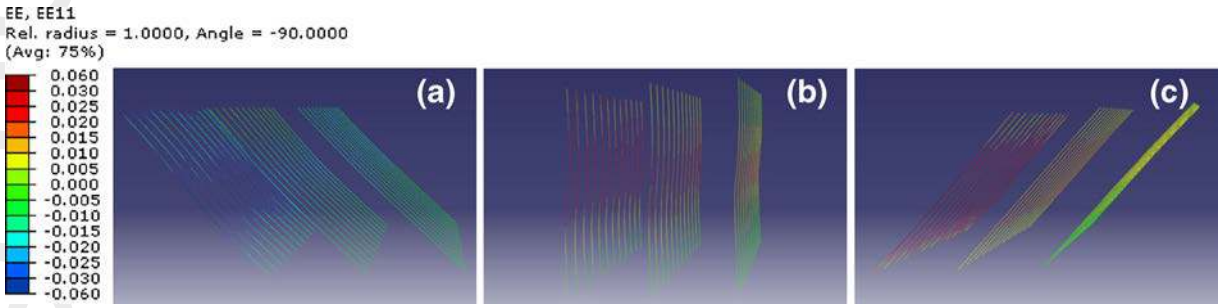


**Fig. 9** Snapshots of root axial strains for a soil strain of 5.0 %, as a function of root orientation and root row. EE11 denotes the normal component of root elastic strain (dimensionless). All the presented cases correspond to roots of the beam type, $E_r$=100 MPa and $\sigma$= 0.5 kPa. (**a c**): three root orientations relative to the shear direction: OD: 45° opposite direction; PD: perpendicular direction; SD: 45° same direction

effect on $\tau_r$ (and therefore root reinforcement) although this effect was different depending on root orientation (Fig. 12d).

With the same $c_s$, i.e. 0.24 kPa, a higher soil friction angle increased the effect of root reinforcement (Fig. 13). Similar $\tau_r - \varepsilon$ curve shapes and tendencies were obtained for both $\phi_s$=30° and $\phi_s$=19°, supporting the use ofweak soil in the present study (Fig. 13). Again, a significant effect of normal pressure on $\tau_r - \varepsilon$ curves was observed in both soils, especially at high soil strain (Fig. 13).

## Discussion

### Complementary use of DEM and FEM approaches

In general, both modelling approaches achieved very consistent results, suggesting a high degree of reliability in our results. Nevertheless, the fact that significant RR occurred at much larger $\varepsilon$ in DEM simulations compared to that of the standard implicit FEM suggests that the frictional interactions between soil and root discrete elements have been more accurately accounted for in the DEM model.

DEM has advantages over standard FEM in several respects. It is based on the modelling of both the soil and the roots as assemblies of interacting bodies whose motion is calculated using classic Newton's law in an updated Lagrangian formulation (Smilauer et al. 2010). This approach allows for explicit calculation of the kinematics at the interface between root and soil discrete elements. In particular, the process of root slippage can be easily accounted for in the DEM, whereas modelling this process in a detailed manner is technically complex and time-consuming using standard implicit FEM modelling. To model soil-root interactions using the FEM, it is equally possible to use the "FRICTION" option that is available in ABAQUS, which mimics more realistic root-soil interface behaviour such as root slippage and separation from soil interface (Yang et al. 2013). By conducting direct shear tests using both "FRICTION" and "EMBEDDED" options, Yang et al. (2013) showed that "EMBEDDED" only slightly underestimated the soil shear strength with respect to frictional behaviour, encountered fewer numerical difficulties and was less time-consuming. This study along with Mickovski et al. (2011) suggest that applying the "EMBEDDED" constraint between root elements and soil elements can be considered a good compromise

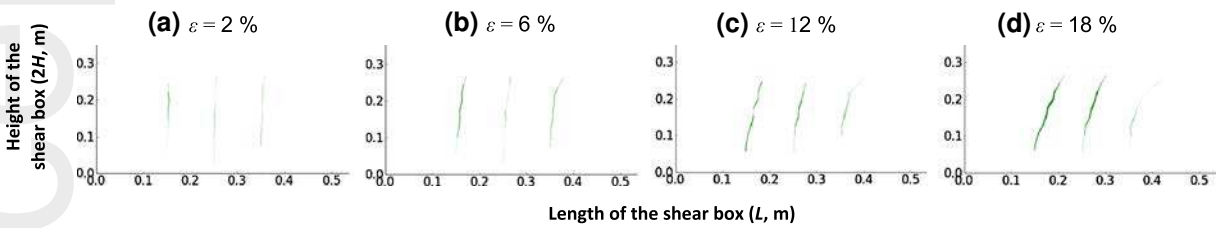


**Fig. 10** Intensity map of the tensile forces of three roots belonging to different rows after Bourrier et al. (2013). Thicker and darker line denotes larger normal forces inside the roots

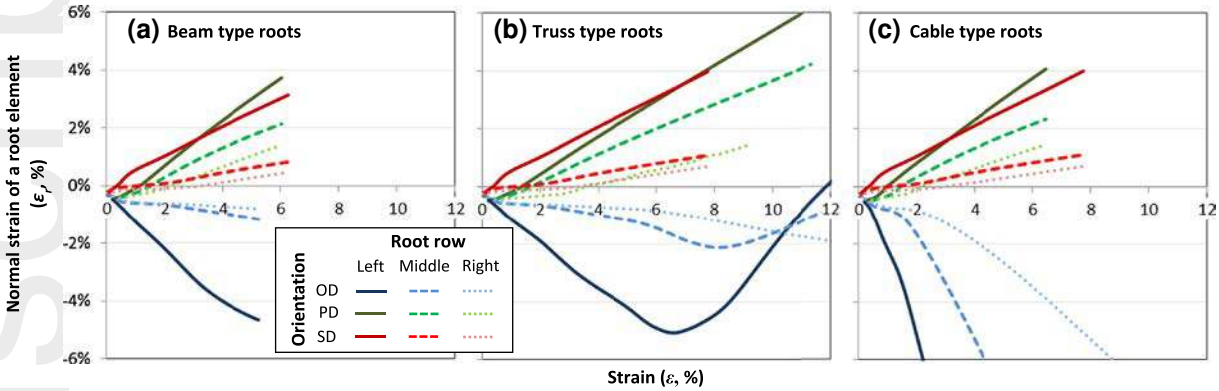


**Fig. 11** Evolution of the elastic axial strains of one root element along soil shear strain, as a function of root row, root orientation and modelled root type. The selected root finite element for plotting is the most central of the 24 elements on the root that is situated in the middle of its row. All the presented cases use roots of $E_r$=100 MPa and $\sigma$=0 5 kPa. Positive and negative values denote roots that are loaded in tension and in compression, respec tively. When roots of cable type (**c**) are loaded in a compression position, they cannot sustain the loading. Root orientation relative to shear direction: OD: 45° opposite direction; PD: perpendicular direction; SD: 45° same direction

between the maintenance of model complexity and generation of satisfactory results. Additionally, the FEM in the form used in this study requires a good mesh quality to prevent simulation convergence problems, whereas

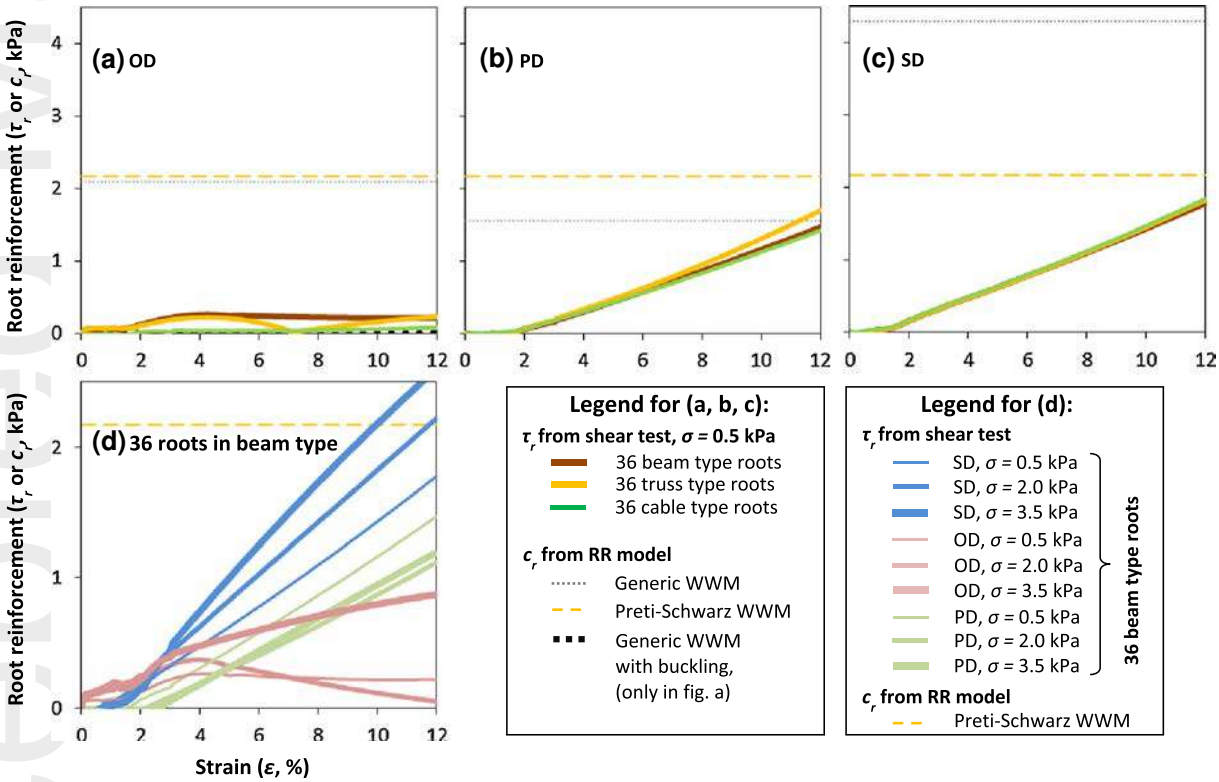


**Fig. 12** Effect of modelled root type, root orientation and normal pressure on root reinforcement ($\tau_r$ or $c_r$) soil strain ($\varepsilon$) curves. $\tau_r$ $\varepsilon$ curves of direct shear tests are based on the FEM. Along the $x$ axis is the strain of the soil (%). (**a c**) three root orientations relative to the shear direction: OD: 45° opposite direction; PD: perpendicular direction; SD: 45° same direction; (**d**): effect of normal pressure with an example of roots of the beam type. Note the different graduations of $y$ axis between (**a c**) and (**d**). In each figure, the estimated $c_r$ using prevailing predictive root reinforce ment models are indicated

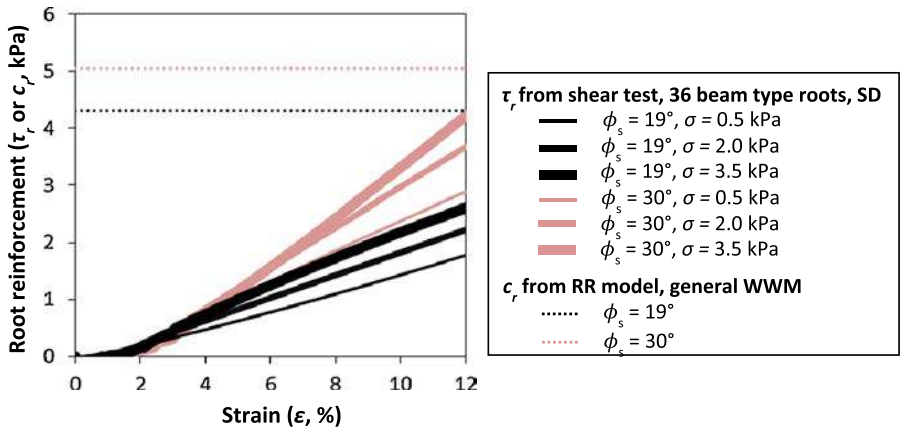


**Fig. 13** Effect of soil friction angle on root reinforcement ($\tau_r$ or $c_r$) soil strain ($\varepsilon$) curves for 36 roots of beam type, 45° orientated in the same direction as the shear direction (SD)

the DEM never encounters mesh-induced convergence problems (being a meshless method). For this reason, the DEM can be used to analyse the mechanisms of root-soil interactions for substantially larger soil strains than the standard FEM, for which convergence problems and loss of accuracy due to the over-distortion of the finite elements occur at large soil strains. This difficulty encountered in standard FEM can however be bypassed using remesh techniques or considering an Eulerian formulation.

Nevertheless, the main drawback of the DEM is the calibration of the different parameters related to soil, roots, and root-soil interactions, which were defined at the local scale of contact between the discrete elements. Little information is available concerning the values of these parameters. Correct and accurate estimation of these parameters requires both experimental validation and/or sensitivity analysis. On the contrary, soil plasticity in FEM based simulations is modelled based on the Mohr-Coulomb criterion for which parameters can be more directly estimated from field data for both rooted and non-rooted conditions (Dupuy et al. 2007; Mickovski et al. 2011). Finally, a single DEM based simulation requires much more robust CPU capacity and more intensive computation than a single FEM based simulation. In order to facilitate computation using the DEM, appropriate scaling of soil and root elements is thus indispensable.

Overall, both modelling methods are appropriate and may be applied for evaluation of the mechanical effects of plants against shallow landslides, incorporating more complex root architectures and loading cases. Both modelling approaches can be used as complementary tools when characterising root reinforcement in the soil matrix. The DEM, which takes into account more exhaustive potential root reinforcement processes provides a good reference to cross validate results from FEM simulations using similar soil and root properties. The validated FEM models can also be used for performing large amounts of simulations, especially when studying the effect of highly variable root traits on soil stress.

## Root efficiency as a function of roots geometry, position, and mechanical traits

Our results showed that the $\tau - \varepsilon$ curves between non-rooted soils and rooted soils shared almost the same values for $\varepsilon < 1.5$ %. Therefore, roots seem to have little influence on soil reinforcement for small strains acting on soil-roots composite. When shear failure occurs, immediate loading of the roots may not be possible due to insufficient motion of soil spheres. This phenomenon may be elevated in non-compacted or weakly cohesive soils or at small/normal pressures, i.e. the cases used here, as the soil strains require larger macroscopic sample strains to propagate through the soil and thus apply load to the roots. Similar conclusions could be drawn from the $\tau - \varepsilon$ curves published by Mickovski et al. (2011) based on FEM simulations and by Ghestem et al. (2013) based on experimental tests (for low normal pressures). Therefore, to increase soil strength at low soil deformation, it would seem to be of little interest to look for "mechanically stronger roots". Instead, it might be of more use to concentrate on gaining soil strength by

improving hydrological conditions [for example, soil water content in Zhang et al. (2010)] or to focus on fine roots that increase stability of soil aggregate (Fattet et al. 2011).

All of our simulations suggested that roots can only be very effective in increasing the residual soil shear strength at large soil strains. This effectiveness was, however, somewhat conditional and significantly affected by root orientation and root position in the sample. In particular, we showed that roots in the OD orientation and in the most distal row to the origin of shear direction had highly restricted effectiveness on reinforcement, despite being mechanically strong. It is to be noted that our results obtained for large soil strains may be biased by the non-homogeneous distribution of the shear strain through the interface as conventionally observed for such strains in direct shear tests. Indeed, for large sample strains, large plastic strains develop on the side of the box from which the force originates and the relative concentration of roots increases on the leeward side.

Once roots are in favourable orientations and positions for soil reinforcement purposes, it is then root mechanical traits that influence the ability of roots to reinforce the soil. This study highlights the importance of root modulus of elasticity ($E_r$), especially since the root tensile strength ($T_r$) did not play a significant role in the tested configuration. We found significantly higher reinforcement efficiency in highly deformed soil for roots possessing higher $E_r$, despite all the roots having equal $T_r$, i.e. 10 MPa. As a result, the value $T_r$ can be considered the roots' ultimate potential reinforcement, whereas $E_r$ determines the roots' efficiency in releasing this potential. Until now, $E_r$ has rarely been quantified and its effect on soil strength has been poorly discussed, as most studies on root mechanical properties have focused on $T_r$. Nevertheless, several studies have highlighted the important role of $E_r$ in slope reinforcement. For example, Waldron (1977) included $E_r$ as one of the major parameters in his root reinforcement model. Schwarz et al. (2010)'s root bundle model gave rise to speculation that root breakage order was determined by root strain rather than root stress, suggesting the importance of quantifying $E_r$. Based on root pull-out experiments, Mickovski et al. (2007) found that increasing $E_r$ induced a significant increase in the peak of pull-out stress. These studies alongside our results support the hypothesis that $E_r$ can play a key role, perhaps even a role more important than that of $T_r$, in influencing the soil-root interaction.

### Tensile loading: an efficient activation process for root reinforcement

A routine point of view is that the RR (root reinforcement) to the soil is mainly due to their tensile strength, especially in the case of finer roots (if root slippage does not occur) (Waldron 1977; Greenway 1987). The efficiency of compression and bending loaded roots in soil reinforcement has been rarely investigated in the literature. The root compression loading process was modelled by Thomas and Pollen-Bankhead (2010), but it was not discussed in the context of evolving soil strains. In this study, we have modelled three different root types (beam, truss and cable) and found that root type entailed significantly different $\tau - \varepsilon$ curves, mainly in the case of OD orientation. Our simulated results thus suggest that considering soil reinforcement by roots under compression and bending loadings in addition to tension is of minor importance (as long as roots are loaded in tension, i.e. for the PD and SD orientations). This confirms that in both orientations, root reinforcement was mainly due to the tension process. For the PD and SD orientation, both beam and truss type roots provided similar reinforcement, i.e. induced similar $\tau - \varepsilon$ curves until the peak value of $\tau$, suggesting that the reinforcement due to bending loading had little impact. This is consistent with the DEM based results in Bourrier et al. (2013) and suggests that the bending process, which has been deemed an essential process in studies on root anchorage against tree fall (Coutts 1983; Danjon et al. 2013), is of less interest for root reinforcement against landslides (at least for the configurations tested). Exceptions may exist in cases when roots penetrate into bedrock, where the bending effect will likely play a significant role against soil mobilisation (Fan and Lai 2013). Roots in SD orientation might be loaded in tension for smaller soil strains than those in PD orientation and this probably explains why roots in SD orientation always showed the most significant increase of $\tau$.

However, when tension induced reinforcement cannot be activated (i.e. the OD orientation), roots loaded in compression can provide reinforcement. In the OD orientation, beam and truss type roots demonstrated increasing $\tau$ for $\varepsilon$<4.0 %, confirming that compression-induced reinforcement was active. On the contrary, cable type roots in the OD orientation had almost no influence on $\tau$.

Roots of similar diameter have been found to be at different stages of tissue development due to their

topological order (Guo et al. 2008). Since tissue development has been supposed to be closely related to root mechanics (Genet et al. 2005, 2010), it is important to quantify the root age and stage of tissue development so as to better understand the proportion of roots acting as beams, trusses and cables in nature. However, due to the limited knowledge and sampling methodologies on roots, the identification of beams, trusses and cables in roots is tedious and subjective, and may even be impossible in practice. This being the case, it is of extreme importance to (i) determine the main direction of potential shear surfaces and (ii) characterise the preferential growth orientation of roots in regard to the potential shear surface. In order to avoid the case of cable type roots in OD orientation, we suggest preferentially growing roots in a fashion that facilitates tension loading when soil shearing occurs. However, this is only possible if the most probable shear surface can be identified with a significant level of certainty, which is, again, difficult in practice.

## Suggestions for the use and improvement of root reinforcement models

Our simulated $\tau - \varepsilon$ curves showed that root reinforcement was closely dependent on soil strain and the FEM and DEM models demonstrated a high accordance on this. Our modelling results also concur with Docker and Hubble (2008), Mickovski and van Beek (2009) and Ghestem et al. (2013), who carried out in situ direct shear tests with real roots and found that root reinforcement occurred after the yield point rather than before. All these results challenge the suitability of using Mohr-Coulomb criterion for soil-roots composite. In particular, they suggest that the RR models fixing of a constant value of additional cohesion during the complete plastic soil strain process may therefore significantly overestimate the shear resistance before the yield point.

In the RR models used in slope stability analyses, the scope of reinforced soil was assumed to be equivalent to the rooting scope. Our simulation results, however, show that the scope of plastified and intact soil was highly variable in time and space. The shear failure did not always occur at the assumed shear plan, but was closely associated with the traits of the embedded roots. Moreover, we found that not all root rows were efficient providing reinforcement against shear, thus suggesting that a root bundle could impose strong restrictions to its neighbouring root bundles. In the existing RR models, several progressive breakage algorithms between root individuals within a root bundle have been introduced and then demonstrated to be realistic. However, so far, the restriction effect between root bundles has not been incorporated in these models. Using the total number of roots without distinguishing effective and non-effective root bundles might lead to an overestimation in quantifying soil resistance. Another important point is that the use of root quantity and root tensile strength for estimating the additional cohesion is based on the assumption that all roots are loaded in tension (except during the buckling process), which is questionable. According to the above results, which show the low contribution of roots in the OD orientation against soil stress, these RR models overestimate the total root contribution.

Regarding $c_r$-estimates, the simplified WWM gave the highest $c_r$-estimates out of all the models, including the generic WWM. This is obviously due to the high value taken for ROF (ROF=1.2). Thomas and Pollen-Bankhead (2010) pointed out that ROF=1.2 was amongst one of the highest values rather than an average following the doctrine of the mean. Future studies should not arbitrarily choose ROF=1.2 without having examined the soil friction angle and root preferential orientation. Besides the non-effective functioning of roots discussed in the above sections, we found that the effective RR remained fairly low even after the yield point ($\varepsilon$ =1.5 %), especially in the OD orientation. This is because no roots failed even after computational divergence in connection to soil failure. Soil failure preceding root failure has equally been reported in both experimental tests, e.g. Docker and Hubble (2008) and modelling tests, e.g. Bourrier et al. (2013). This suggests that when roots are embedded in soil, they cannot be fully loaded to their ultimate tensile strength ($T_r$). Hence, using $T_r$ in RR models is a questionable choice. Compared to the conventional tension and compression based RR models, only taking into account the buckling effect for the OD oriented roots tended to provide a $c_r$ that was too conservative, suggesting that this mechanical process (if it exists), might not significantly contribute to the RR.

We found equally that normal pressure on the upper shear box significantly affected $\tau_r$ - $\varepsilon$ curves and that its influence was different depending on root orientation. Yet this again is not always considered in RR models which assume that root reinforcement is independent of normal pressure. In nature, roots are located in different soil layers that are subjected to variable loadings due to

soil gravity. We supposed that the increasing loading for increasing soil depth can generally result in a positive effect towards the roots' reinforcement efficiency. The extent to which normal pressure affects root reinforcement should be explored and this effect factored into future RR models.

## Conclusion and perspectives

Through the means of modelling direct shear tests using both standard FEM and DEM based models, this study has aimed to evaluate root reinforcement. Both of these numerical modelling approaches achieved, in general, comparable results. We have showed both advantages and drawbacks for each approach and thus recommend using both of them as complementary tools in future studies.

Based on a simple model design, i.e. embedment of parallel root rows in a homogenous soil medium, we have revealed a high complexity in soil–root interactions during the soil shear process. The apparent root reinforcement to soil stress varied as a function of soil strain and was closely related to root geometry, position in the soil, and mechanical traits. Existing RR models tended to provide higher $c_r$-estimates than those achieved by numerical direct shear tests. We suggest taking into account the effect of root orientation, position, root type and normal pressure in the existing RR models in order to enhance both their accuracy of prediction and their accordance with the modelled or observed processes.

**Acknowledgments** This study was financed by a joint research program Ingecotech CNRS/Irstea project CATARS (Characterisation of Architectural Traits of Root Systems in the Processes of Soil Stabilisation) and a French funded ANR project ECOSFIX (Ecosystem Services of Roots Hydraulic Redistribution, Carbon Sequestration and Soil Fixation, ANR 2010 STRA 003 01). We are grateful to Dr. Alexia Stokes (INRA, UMR AMAP, France) and Huaxiang Zhu (IRSTEA, France) for their inspiring suggestions to this work. Thanks are also due to François Kneib (IRSTEA, France) and Jean Baptiste Barré (IRSTEA, France) for their technical support with regard to numerical modelling. Finally, we thank Marie Christou Kent (Université Joseph Fourier, France) for checking the manuscript's English.

## References

Abe K, Iwamoto M (1985) Effect of tree roots on soil shearing strength. In International Symposium on Erosion, Debris Flow and Disaster Prevention, Tsukuba, Japan, pp 341 345

Bischetti GB, Chiaradia EA, Simonato T, Speziali B, Vitali B, Vullo P, Zocco A (2005) Root strength and root area ratio of forest species in Lombardy (northern Italy). Plant Soil 278:11 22

Bischetti GB, Chiaradia EA, Epis T, Morlotti E (2009) Root cohesion of forest species in the Italian Alps. Plant Soil 324:71 89

Bourrier F, Kneib F, Chareyre B, Fourcaud T (2013) Discrete modeling of granular soils reinforcement by plant roots. Ecol Eng 61:646 657

Burylo M, Rey F, Roumet C, Buisson E, Dutoit T (2009) Linking plant morphological traits to uprooting resistance in eroded marly lands (Souhern Alps, France). Plant Soil 324:31 42

Cohen D, Schwarz M, Or D (2011) An analytical fiber bundle model for pullout mechanics of root bundles. J Geophys Res Earth Surface (2003 2012) 116:F3

Coutts MP (1983) Root architecture and tree stability. Plant Soil 71:171 188

Cundall P, Strack O (1979) Discrete numerical model for granular assemblies. Geotechnique 29(1):47 65

Danjon F, Barker DH, Drexhage M, Stokes A (2008) Using three dimensional plant root architecture in models of shallow slope stability. Ann Bot 101:1281 1293

Danjon F, Khuder H, Stokes A (2013) Deep phenotyping of coarse root architecture in *R. pseudoacacia* reveals that tree root system plasticity is confined within its architectural model. PLoS ONE 8(12): e83548. doi:10.1371/journal.pone.0083548

Docker BB, Hubble TCT (2008) Quantifying root reinforcement of river bank soils by four Australian tree species. Geomorphology 100:401 418

Donald IB, Zhao T (1995) Stability analysis by general wedge methods. In The Ian Boyd Donald Symposium on ModernDevelopments in Geomechanics, Monash University, Melbourne, Haberfield CM (ed.). Monash University; pp 1 28

Dupuy L, Fourcaud T, Stokes A (2005a) A numerical investigation into the influence of soil type and root architecture on tree anchorage. Plant Soil 278:119 134

Dupuy L, Fourcaud T, Stokes A (2005b) A numerical investigation into factors affecting the anchorage of roots in tension. Eur J Soil Sci 56:319 327

Dupuy L, Fourcaud T, Lac P, Stokes A (2007) A generic 3D finite element model of tree anchorage integrating soil mechanics and real root system architecture. Am J Bot 94:1506 1514

Fan CC, Chen YW (2010) The effect of root architecture on the shearing resistance of root permeated soils. Ecol Eng 36(6): 813 826

Fan CC, Lai YF (2013) Influence of the spatial layout of vegetation on the stability of slopes. Plant Soil 1 13

Fan CC, Su CF (2008) Role of roots in the shear strength of root reinforced soils with high moisture content. Ecol Eng 33(2): 157 166

Fattet M, Fu Y, Ghestem M, Ma WZ, Foulonneau M, Nespoulos J, Le Bissonnais Y, Stokes A (2011) Effects of vegetation type on soil resistance to erosion: relationship between aggregate stability and shear strength. Catena 87:60 69

Fourcaud T, Ji JN, Zhang ZQ, Stokes A (2008) Understanding the impact of root morphology on overturning mechanisms: a modelling approach. Ann Bot 101(8):1267 1280

Frydman S, Operstein V (2001) Numerical simulation of direct shear of root reinforced soil. Ground Improv 5:41 48

Genet M, Stokes A, Salin F, Mickovski SB, Fourcaud T, Dumail JF, van Beek R (2005) The influence of cellulose content on tensile strength in tree roots. Plant Soil 278:1 9

Genet M, Kokutse N, Stokes A, Fourcaud T, Cai XH, Ji JN, Mickovski S (2008) Root reinforcement in plantations of *Cryptomeria japonica* D. Don: effect of tree age and stand structure on slope stability. For Ecol Manage 256:1517 1526

Genet M, Stokes A, Fourcaud T, Norris JE (2010) The influence of plant diversity on slope stability in a moist evergreen decid uous forest. Ecol Eng 36:265 275

Ghestem M, Veylon G, Bernard A, Vanel Q, Stokes A (2013) Influence of plant root system morphology and architectural traits on soil shear resistance. Plant Soil 1 19

Gray DH, Leiser AT (1982) Biotechnical Slope Protection and Erosion Control. Van Nostrand Reinhold Company, New York

Gray DH, Ohashi H (1983) Mechanics of fiber reinforcement in sand. J Geotech Eng ASCE 109(3):335 353

Gray DH, Sotir RB (1996) Biotechnical and soil bioengineering slope stabilization. John Wiley & Sons, New York

Greenway DR (1987) Vegetation and slope stability. In: Stability S (ed) Chapter 6. John Wiley & Sons Ltd., Chichester, pp 187 230

Greenwood JR (2006) SLIP4EX a program for routine slope stability analysis to include the effects of vegetation, rein forcement and hydrological changes. Geotech Geol Eng 24: 449 465

Guo DL, Xia M, Wei X, Chang W, Liu Y, Wang Z (2008) Anatomical traits associated with absorption and mycorrhizal colonization are linked to root branch order in twenty three Chinese temperate tree species. New Phytol 180: 673 683

Hales TC, Ford CR, Hwang T, Vose JM, Band LE (2009) Topographic and ecologic controls on root reinforcement. J Geophys Res: Earth Surf (2003 2012) 114:F3

Hathaway RL, Penny D (1975) Root strength in some *Populus* and *Salix* Clones. N Z J Bot 13(3):333 344

Ji J, Kokutse N, Genet M, Fourcaud T, Zhang Z (2012) Effect of spatial variation of tree root characteristics on slope stability. A case study on Black Locust (*Robinia pseudoacacia*) and Arborvitae (*Platycladus orientalis*) stands on the Loess Plateau, China. Catena 92:139 154

Kokutse NK (2008) Modélisation du renforcement des sols et analyse numérique de l'impact de la structure des peuplements forestiers sur la stabilité des pentes. Applications à l'éco ingénierie. [Modellling of soil reinforce ment and numerical analysis of impact of forest stand struc ture on slope stability. Application to eco engineering]. PhD thesis, Université Bordeaux 1

Lin DG, Huang BS, Lin SH (2010) 3 D numerical investigations into the shear strength of the soil root system of Makino bamboo and its effect on slope stability. Ecol Eng 36:992 1006

Mao Z, Saint André L, Genet M, Mine FX, Jourdan C, Rey H, Courbaud B, Stokes A (2012) Engineering ecological pro tection against landslides in diverse mountain forests: choos ing cohesion models. Ecol Eng 45:55 69

Mao Z, Jourdan C, Bonis ML, Pailler F, Rey H, Saint André L, Stokes A (2013) Modelling root demography in heterogeneous mountain forests and applications for slope stability analysis. Plant Soil 363:357 382

Mao Z, Bourrier F, Stokes A, Fourcaud T (2014) Three dimen sional modelling of slope stability in heterogeneous montane forest ecosystems. Ecol Model 273:11 22

Mattia C, Bischetti GB, Gentile F (2005) Biotechnical character istics of root systems of typical Mediterranean species. Plant Soil 278:23 32

Mickovski SB, van Beek LPH (2009) Root morphology and effects on soil reinforcement and slope stability of young vetiver (*Vetiveria zizanioides*) plants grown in semi arid cli mate. Plant Soil 324(1 2):43 56

Mickovski SB, Bengough AG, Bransby MF, Davies MCR, Halett PD, Sonnenberg R (2007) Material stiffness branching pat tern and soil matric potential affect the pullout resistance of model root systems. Eur J Soil Sci 58:1471 1481

Mickovski SB, Stokes A, van Beek R, Ghestem M, Fourcaud T (2011) Simulation of direct shear tests on rooted and non rooted soil using finite element analysis. Ecol Eng 37:1523 1532

Pollen N, Simon A (2005) Estimating the mechanical effects of riparian vegetation on stream bank stability using a fiber bundle model. Water Resour Res 41, W07025. doi:10.1029/2004WR003801

Pollen N, Simon A, Collison A (2004) Advances in assessing the mechanical and hydrologic effects of riparian vegetation on streambank stability. Riparian Vegetation Fluvial Geomorp Water Sci Appl 8:125 139

Preti F, Giadrossich F (2009) Root reinforcement and slope bioengineering stabilization by Spanish Broom (*Spartium junceum* L.). Hydrol Earth Syst Sci 13: 1713 1726

Preti F, Schwarz M (2006) On root reinforcement modelling. In: Geophysical Research Abstracts, vol. 8, 2006, The role of vegetation in slope stability and mitigation measures against landslides and debris flows, EGU General Assembly 2006, April 2 7, 2006

Reubens B, Poesen J, Danjon F, Geudens G, Muys B (2007) The role of fine and coarse roots in shallow slope stability and soil erosion control with a focus on root system architecture: a review. Trees 21(4):385 402

Sakals ME, Sidle RC (2004) A spatial and temporal model of root cohesion in forest soils. Can J For Res 34:950 958

Schmidt KM, Roering JJ, Stock JD, Dietrich WE, Montgomery DR, Schaub T (2001) The variability of root cohesion as an influence on shallow landslide susceptibility in the Oregon Coast Range. Can Geotech J 38:995 1024

Schwarz M, Lehmann P, Or D (2010) Quantifying lateral root reinforcement in steep slopes from a bundle of roots to tree stands. Earth Surf Process Landf 35:354 367

Shibuya S, Mitachi T, Tamate S (1997) Interpretation of direct shear box testing of sands as quasi simple shear. Geotechnique 47:769 790

Simon A, Curini A, Darby S, Langendoen E (1999) Streambank mechanics and the role of bank and near bank processes in incised channels. In: Darby S, Simon A (eds) Incised River Channels. Wiley, New York, pp 123 152

Smilauer V, Catalano E, Chareyre B, Dorofeenko S, Duriez J, Gladky A, Kozicki J, Modenese C, Scholtes L, Sibille L, Stransky J, Thoeni K (2010) Yade documentation, 1st edn. The Yade Project, http://yade dem.org/doc/

Stokes A, Atger C, Bengough AG, Fourcaud T, Sidle RC (2009) Desirable plant root traits for protecting natural and engineered slopes against landslides. Plant Soil 324:1 30

Thomas RE, Pollen Bankhead N (2010) Modeling root reinforce ment with a fiber bundle model and Monte Carlo simulation. Ecol Eng 36:47 61

Thornton C, Zhang L (2003) Numerical simulations of the direct shear test. Chem Eng Technol 26(2):153 156

Waldron LJ (1977) The shear resistance of root permeated homogeneous and stratified soil. Soil Sci Soc Am J 41:843 849

Wu TH (1976) Investigation of Landslides on Prince of Wales Island, Alaska. Ohio State University, Department of Civil Engineering, Geotechnical Engineering Report 5, pp 94

Wu TH, Watson A (1998) In situ shear tests of soil blocks with roots. Can Geotech J 35(4):579 590

Wu TH, McKinnell WP, Swanston DN (1979) Strength of tree roots and landslides on prince of wales lsland Alaska. Can Geotech J 16:19 33

Yang M, Défossez P, Fourcaud T (2013) Improving finite element models of roots soil mechanical interactions. Proceedings of the 7th International Conference on Functional Structural Plant Models, Saariselkä, Finland, 9 14 June 2013. Eds. Risto Sievänen, Eero Nikinmaa, Christophe Godin, Anna Lintunen & Pekka Nygren. http://www.metla.fi/fspm2013/proceedings. ISBN 978 951 651 408 9

Zhang CB, Chen LH, Liu YP, Ji XD, Liu XP (2010) Triaxial compression test of soil root composites to evaluate influ ence of roots on soil shear strength. Ecol Eng 36:19 26